Int J Syst Assur Eng Manag
https://doi.org/10.1007/s13198-023-01916-1

ORIGINAL ARTICLE

# Optimization of wire electro discharge machining parameters using principal component analysis

**C. Senthilkumar**[1] · **C. Nandakumar**[2]

Received: 26 February 2021 / Revised: 12 January 2022 / Accepted: 6 April 2023


**Abstract** Titanium and its alloys are commonly utilized in the aerospace and automobile sectors, because of its superior corrosion resistance, chemical inertness, strength properties. Machining of Titanium alloys using traditional method is extremely challenging task due to it has low thermal conductivity, poor electrical conductivity, quick strain hardening, high cutting tool temperatures, poor surface quality, and built-up edge formation. Hence, Nontraditional machining methods, like WEDM, can overcome these technical challenges and produce complicated part forms with good surface polish with high precision. Hence, the current study focuses on how process variables affect the responses like rate of removal (RR) and roughness (Ra). Because WEDM is an extremely complicated stochastic process, even an incidental variations in one of control factors can cause the responses to change, choosing an appropriate process parameter combination is vital. As a result, to cater the needs of today's industrial technology and customers, a thorough investigation into the choosing appropriate process parameters and solutions is required. So, multi-objective optimization based on principal component analysis (PCA) was used to optimize the process parameters.

**Keywords** Removal rate · Ra · PCA

✉ C. Senthilkumar
csmfgau@gmail.com

[1] Department of Mechanical Engineering, University College of Engineering, Panruti, India

[2] Department of Production Technology, MIT Campus, Anna University, Chennai -44, India

## 1 Introduction

Due to excellent corrosion resistance and strength-to-weight ratio, titanium alloys (Ti) have recently become popular in a variety of industries, including automobiles, space vehicles, chemical and electronic industry, biomedical field. Traditional methods of machining titanium alloy are significantly hampered by speed limitations, heavy tool wear, and chipping (Oliver Nesa Raj and Prabhu, 2017). Nontraditional machining methods, like WEDM are utilised as an alternative machining method for titanium alloy to overcome the constraints. In WEDM material removed by discharging a succession of repetitive pulses between both the Ti alloy and a travelling electrode encased in a distilled water, extremely high temperature is generated (approximately about 20,000 °C) in the area where electric discharge ensues in order to melt and erode the surface with best precision and accuracy, the debris formed are evacuated in the gap by flowing dielectric. In this proces no cutting force, mechanical strains, chatter or vibration issues, because electrode and the work piece are not in direct interaction (Alduroobi and colleagues, 2020). Wire wear is a huge issue in the WEDM process. Wire wear could not produce required geometrical dimensions in most WEDM processes, and tool costs account for roughly 70% of total operation costs. Component quality is established by the alloy's surface finish, which is a crucial design component to consider for attributes like as fatigue strength and wear resistance. Nonetheless, traditional brass electrodes and coated brass electrodes can achieve excellent dimensional precision but have a low removal rate due to electrode degradation. However, electrode coated with zinc and treated with liquid nitrogen to improve the various properties and dimensional stability of the electrode (Ashish Goyal2017). Significant contributions have been found to assessing the outcome of liquid nitrogen

Published online: 17 April 2023

cooling of electrode on various materials during machining. Goswami and Kumar (2014) used untreated coated wire and liquid nitrogen cooled coated wire for WEDM of Inconel. The analysis found that cooling with liquid nitrogen improved the WEDM process. The most critical factors that impact machining performance were found after cryogenic treatment of electrode. WEDM with cryogenic treated brass wire was used to machine EN-31 steel was investigated by Kapoor et al. (2015). Deep cryogenic treatment improved WEDM machining performance by increasing refined grains and electrical conductivity. Additional wire treatment, pulse duration, and wire tension have all been identified as critical factors in maximizing MRR. Cutting performance of HSLA with untreated and cryogenically treated brass wire was investigated by Tahir et al. (2019). Among this, treated brass wire performs better than untreated brass wire for machining, according to their research. Inconel 718 work piece treated with liquid nitrogen using Bronco cut-Wire were examined by Nayak and Mahapatra (2016). During the WEDM tapering process, various factors were revealed to be key criteria for angular inaccuracy. The angular inaccuracy was decreased because the workpiece and wire were cryogenically treated. To determine the correlation between various factors affecting the performance features ANN model was established. Vázquez-Méndez et al. (2020) estimated a model for forming a bypass for railways for efficient and economic way to avoids the urban region and nearby structures, which is a critical challenge in railway engineering. The estimated model could be incredibly constructive tool intended for engineers dealing with similar issues. Aliakbar Hasani et al. (2021) proposed a model for a global product manufacturing system that takes economically and environmentally effects into consideration when establishing the infrastructure and use remedial measures to develop a robust supply chain system. A unique hybrid methodology is devised that comprises an augmented strength Pareto evolutionary technique to deal with computing flexibility of this multi-objective optimization issue. The proposed optimization network can adapt to the demands of its global clients in a flexible and environmental friendly manner. It was discovered that there was a substantial volume of literature accessible in the field of WEDM with cryogenic treated various electrode and workpiece. Further in the literature study, optimization of WEDM parameter process with cryogenic treated electrode was scarce. WEDM responses are independent of each other and traditional optimization approach would not correlate the response may lead to imprecise results. Nonetheless, the multiobjective optimization employing response surface has received little attention. To address this gap, this research explores a multi-response outcome using a DOE mixed array and a principal component analysis (PCA) approach. PCA differs from most other techniques in that it obtains the mean and variance equations using the dispersion of error concept.

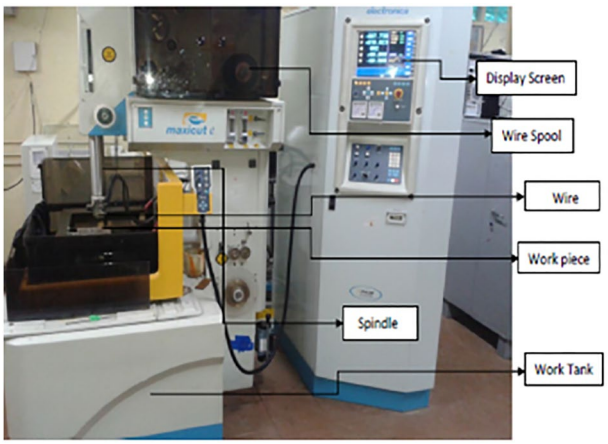


**Fig.1** Maxicut e WEDM machine

**Table 1** Process parameters and their levels

| Parameters | Level | | |
|---|---|---|---|
| | -1 | 0 | -1 |
| Current, amp (A) | 6 | 9 | 12 |
| Pulse on time, μs (B) | 60 | 90 | 120 |
| Pulse off time, μs(C) | 100 | 150 | 200 |

This is written with the most significant principal component scores and is computed that used a regulated noise response surface model that can be used to replace the existing correlated dataset. Furthermore, when giving weights to quality traits that are linked to other quality aspects, PCA must eliminate ambiguity and complexity in engineers' assessments. By translating several responses into a single index, PCA transforms multi-objective optimization into a solitary optimization (Walia et al. 2006). Hence, in this study, operating parameters were modified using Principal component analysis (PCA) in order to maximize MRR and diminish Ra.

## 2 Experimental work

In this study, a CNC WEDM was used to execute machining using distilled water as the dielectric fluid as shown in Fig. 1. Titanium grade 5 (Ti-6Al-4 V) plates of 3 mm thick were considered as workpiece and zinc coated brass wire of 0.25 mm thick was electrode. Controllable factors and their ranges were indicated in Table 1. The wire electrode is continuously passed through a hollow copper tube setup consisting of a stainless steel box with thermo coal in which nitrogen is maintained at -196 °C for continuous cooling of the electrode during the WEDM process, as shown in Fig. 2. Based on Box Benhen design, experiments were accomplished and the responses were recorded which is

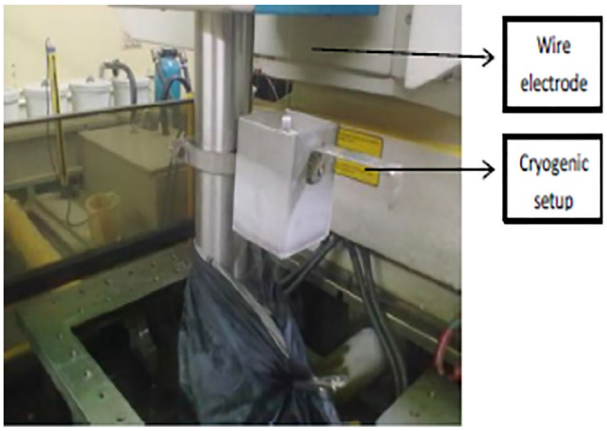


**Fig. 2** Cryogenic setup mounted on WEDM machine

**Table 2** Experimental data

| Sl no | Current, (amp) | Pulse on time, (μs) | Pulse off time, (μs) | MRR (mg/min) | Ra, (μm) |
|---|---|---|---|---|---|
| 1 | 6 | 60 | 150 | 0.0544 | 1.27 |
| 2 | 12 | 60 | 150 | 0.0599 | 2.97 |
| 3 | 6 | 120 | 150 | 0.0563 | 1.59 |
| 4 | 12 | 120 | 150 | 0.0681 | 2.76 |
| 5 | 6 | 90 | 100 | 0.0536 | 1.08 |
| 6 | 12 | 90 | 100 | 0.0599 | 2.69 |
| 7 | 6 | 90 | 200 | 0.0574 | 1.75 |
| 8 | 12 | 90 | 200 | 0.0563 | 2.63 |
| 9 | 9 | 60 | 100 | 0.0535 | 1.95 |
| 10 | 9 | 120 | 100 | 0.0589 | 1.28 |
| 11 | 9 | 60 | 200 | 0.0578 | 1.11 |
| 12 | 9 | 120 | 200 | 0.0602 | 1.05 |
| 13 | 9 | 90 | 150 | 0.0569 | 1.62 |
| 14 | 9 | 90 | 150 | 0.0569 | 1.62 |
| 15 | 9 | 90 | 150 | 0.0569 | 1.62 |

disclosed in Table 2. The variation of weight was divided by the constant time of WEDM to assess the Removal Rate (RR). SJ-210 surface roughness analyzer, surface roughness (Ra) was measured three times and the average has been used to evaluate surface roughness for each specimen. The machined surfaces were evaluated after WEDM process has been investigated through SEM.

## 3 Results and discussion

### 3.1 Parametric influence on RR

Figure 3 depicts the impact of current on RR. It is perceived that with a rise in current, the RR is shown to increase.

**Table 3** Normalized and weighted normalized matrix

| Experiment number | Normalized matrix | |
|---|---|---|
| | MRR (gm/min) | Ra, (μm) |
| 1 | 0.134328 | 0.885417 |
| 2 | 0.955224 | 0 |
| 3 | 0.41791 | 0.71875 |
| 4 | 2.179104 | 0.109375 |
| 5 | 0.014925 | 0.984375 |
| 6 | 0.955224 | 0.145833 |
| 7 | 0.58209 | 0.635417 |
| 8 | 0.41791 | 0.177083 |
| 9 | 0 | 0.53125 |
| 10 | 0.80597 | 0.880208 |
| 11 | 0.641791 | 0.96875 |
| 12 | 1 | 1 |
| 13 | 0.507463 | 0.703125 |
| 14 | 0.507463 | 0.703125 |
| 15 | 0.507463 | 0.703125 |

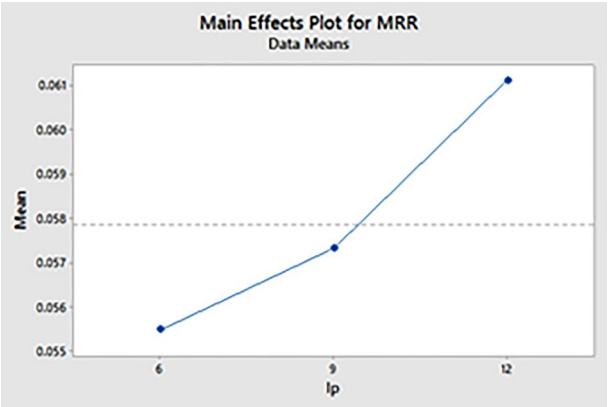


**Fig. 3** RR at varying current

Higher current (9 to 12 amps) results in greater penetration of discharge sparks into the workpiece surface, culminating in high-pressure vapour cavitation bubbles inside, which gradually build up due to extensive melting and vaporisation of the workpiece and electrode rapid discontinuation of discharge results in aggressive blow of vapour sphere, expelling molten material into the dielectric, amplifying RR. Because the energy density within the vapour bubble is lower for lesser current values of 6 to 9 amps, the quantity melted is smaller, resulting in a lower RR (Jabbaripour et al. 2012). The effect of on time on RR is depicted in Fig. 4. RR declines, when the pulse on time is climbed from 60 to 90 μs. This would be due to the drop in plasma channel diameter, which diminishes energy density during WEDM, resulting in less discharge energy transfer to a workpiece and a lower RR. Increase the pulse on time from 90 μs to 120 μs,

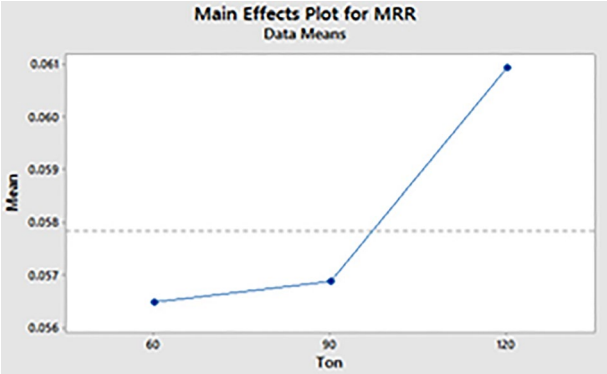


**Fig. 4** RR at varying pulse on time

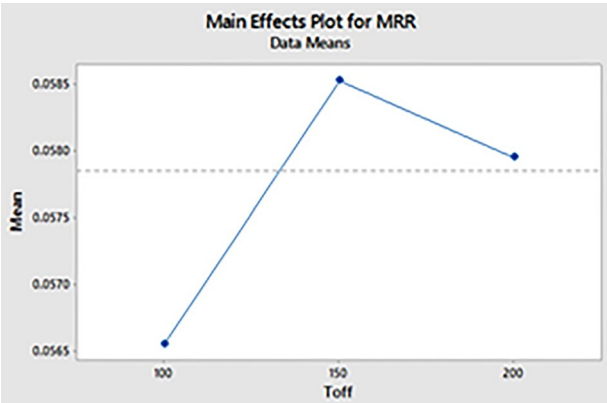


**Fig. 5** RR at varying pulse off time

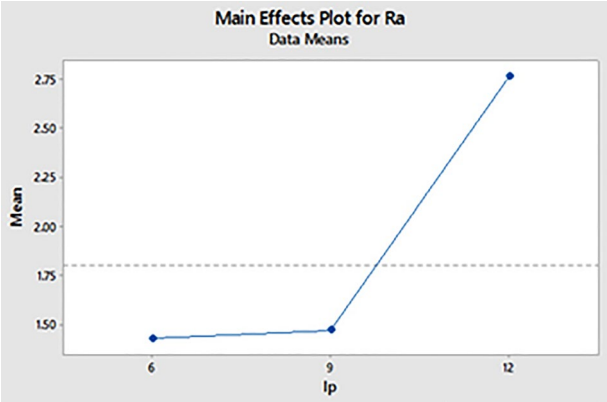


**Fig. 6** Ra at varying current

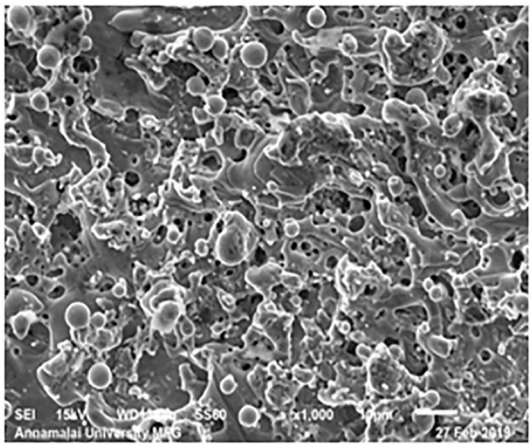

**Fig. 7** Small and shallow craters obtained at lower current

the diameter of the discharge column rises, more positive ions approach towards the workpiece, spark with high intensity intruded on the workpiece increase melting, vaporization of workpieceduring machining, resulting in higher RR (Senthilkumar and Ganesan 2015). Figure 5 illustrates the variation of pulse off time with MRR. At lower pulse off time, effective machining happens as sparking efficiency improves, and debris evacuated swiftly from the gap, and fresh dielectric fluid is injected, resulting in a higher RR (Sanjeev Kumar et al. 2017). However, RR from the other hand, diminishes as pulse off time grows from 150 µs to 200 µs. Longer pulse off time reduces the plasma channel, diminishing the attack of positive ions on the workpiece. Further, the number of sparks intruding on the surface in a particular time is reduced; shrinking the size of the crater developed on the machined surface and leads to lower RR.

### 3.2 Parametric influence on Ra

The function of current on surface roughness is depicted in Fig. 6. Ra seems to have a lower increasing trend from 6 to 9A. It is because discharge energy is lower at lower current values, resulting in a smaller thermal effect, which inhibits the removal rate and provides more uniform smooth craters on the surface, as seen in Fig. 7 (Torreset al. 2017). From 9 to 12A, Ra increases exponentially. Higher current is expected to generate more thermal energy in the gap, causing stern cracking of the dielectric to happen more frequently, leading to the formation of a molten pool that is becoming overheated. This molten metal condenses onto gas bubbles since it evaporates. When the charge stops, the gas bubbles shatter, expelling the molten metal from the surface of the Ti alloy. The development of crater is determined by the gas bubbles that erupt during machining. Air bubbles become trapped in the melted region as the remaining molten Ti alloy freezes on the machined surface, resulting in micro gaps on the surface, as illustrated in SEM micrograph Fig. 8. (Rajeshet al. 2012). Figure 9 depicts the impact of on time on surface roughness. Surface roughness of the Ti alloy grows from the 60 to 90 µs, indicating that the violent spark produces excessive melting, results in lowering plasma channel cleansing efficiency, due to plasma

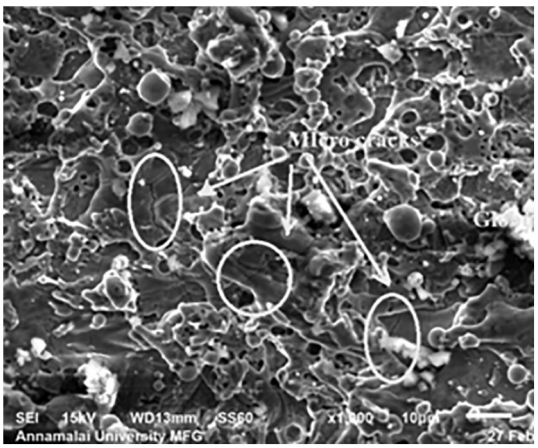


**Fig. 8** Micro-cracks and holes, globules obtained at high current

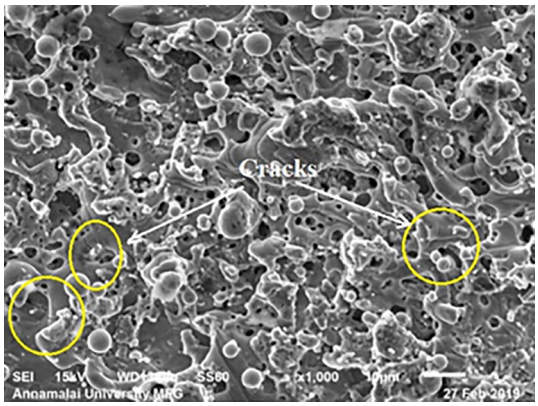


**Fig. 10** Crack and crater formation population are reduced at higher pulse on time

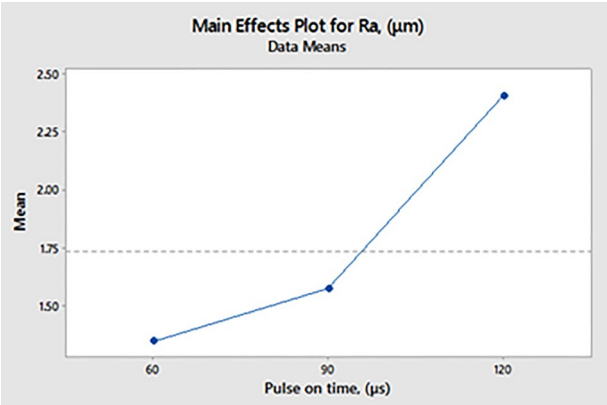


**Fig. 9** Ra at varying pulse on time

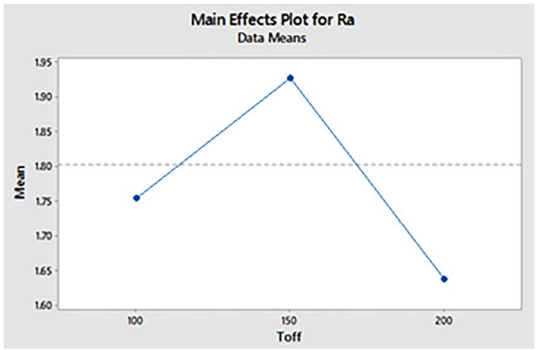


**Fig. 11** Ra at varying pulse off time

channel enlargement. As a result, the dielectric removed a small fraction of debris and melt, and the remaining molten Ti melt generated a recast layer on the Ti surface, ruining the surface. Due to the rapid growth of the plasma channel, which snatched away a significantly greater amount of material from the top layers of Ti alloy as the pulse on time grows to 120 µs from 90 µs, the focus of spark energy increases, resulting in surface aberrations such as globules and micro voids becoming somewhat prominent. When an electrical spark reaches a temperature of above 10,000 °C, which is high enough to melt and evaporate the metal but not high enough to withstand high exploding pressure, which can splatter all of the melted material from the surface, micro holes and craters form, resulting in an irregular surface as can be seen in Fig. 10 (Barenji et al. 2016). Figure 11 shows a correlative plot of off time vs surface roughness. The graph depicts that as the off time climbs from 100 to 150 µs, there has been inadequate time to empty the melted Ti alloy out of the gap, culminating in electrode short-circuiting. As a consequence, the population of craters was expanded to cover the full surface and highly populated colony of deep craters. This in turn decline surface finish (Rahul et al. 2019). As the pulse off time extends, the idle duration prolongs, permitting the debris to be washed out much more efficiently, resulting in a decline in Ra (Bharat et al. 2017). Additionally, the extended off time imparted lower heat energy, resulting in reduced Ti alloy attrition and flushed out, resulted in a smooth surface. (Chalisgaonkar and Kumar 2014).

## 4 Principal component analysis

The technique of maintaining a balance between two or more responses is referred to as multi optimization. The suitability of a solution is impacted by a number of variables, including the customer's needs and wants as well as the problem context. Two objectives have been investigated in the present study, particularly MRR and Ra. It has also been noticed that the MRR grows; surface roughness goes up as well. Nevertheless, our goal is to maximize MRR despite lowering Ra. Since these goals are incompatible, a single correct solution will not satisfy. As a result, the method was optimized using

principal component analysis (PCA), which uses linear permutation to maintain as much different information as feasible. Pearson (1901) proposed PCA, a multivariate statistical method that was subsequently improved by Hotelling (1933). Multiple correlated replies are decomposed into a number of unrelated quality factors. Following that, all of the outcome measurements are assembled to obtain arithmetic function, which is composite principal component (CPC) and shows the ultimate quality. In order to estimate the CPC depending on the total quality metrics, the composite principal component is maximized. Finally, to estimate the CPC based on the system's accuracy enhancing, the combined principal component is maximized. PCA collect all the performance measures and different dimensions of the system by data preprocessing. Procedure for employing PCA is given below:

Step 1: Arrange the many performance parameters that were measured during machining as shown by Eq. (1).

$$R = \begin{pmatrix} X_{11} & X_{12} & . & . & X_{1N} \\ X_{21} & X_{22} & . & . & X_{2N} \\ . & . & . & . & . \\ . & . & . & . & . \\ X_{M1} & X_{M2} & . & . & X_{MN} \end{pmatrix} \tag{1}$$

where X is the number of trials, and output R quantify of ith alternative on jth condition.

Step II: Normalization refers to the process of converting the decision matrix's original output to a range of values between 0 and 1. Three types of data normalisation procedures are utilised to portray the data: lesser is better (LB) and larger is better (LB). The performance parameters of greater is better (GB) and lesser is better (LB) are employed in this study. The normalised output matrix of n trials with m characteristics is calculated by Using Eqs. 2 and 3:

For ''larger is better"

$$U_{ij} == \frac{Xi(\mu) - \min Xi(\mu)}{\max Xi(\mu) - \min Xi(\mu)} \tag{2}$$

For ''lesser is better"

$$U_{ij} == \frac{\max \mathrm{Xi(k)} - \mathrm{Xi(k)}}{\max Xi(\mathrm{k}) - \min Xi(k)} \frac{\max \mathrm{Xi(k)} - \mathrm{Xi(k)}}{\max Xi(\mathrm{k}) - \min Xi(k)} \tag{3}$$

where Ui($\mu$) is the standardized assessment of output $\mu$, min Xi($\mu$) smallest value for the $\mu$ th outcome, and max Xi($\mu$) biggest value for the $\mu$ th outcome. Equation 4 indicates that U is the standardized array (4).

$$U = \begin{pmatrix} U_{11} & U_{12} & . & . & U_{1N} \\ U_{21} & U_{22} & . & . & U_{2N} \\ . & . & . & . & . \\ . & . & . & . & . \\ U_{M1} & U_{M2} & . & . & U_{MN} \end{pmatrix} \tag{4}$$

Step III: From the normalized variance- and covariance matrix obtained as Z as follows

$$Z = \begin{pmatrix} N_{11} & N_{12} & . & . & N_{1N} \\ N_{21} & N_{22} & . & . & N_{2N} \\ . & . & . & . & . \\ . & . & . & . & . \\ N_{M1} & N_{M2} & . & . & N_{MN} \end{pmatrix} \tag{5}$$

$$N_{k,l} = \frac{Cov\left[Ui(o), Uip\right)}{\sqrt{Var}Ui(ko) \times VarUi(o)} \tag{6}$$

where, 1= 1,2,3,..., O and Cov *Ui(o), Vi(p)* is the covariance of*Ui(o),Vi(p).*

Step V: Evaluate major components of j.

Step IV: Eigen values and Eigen vectors were calculated with the aid of variance and covariance using Eq. 6.

Step V: The eigenvector Yj denotes the weighting factor for the jth principal component's j number of performance attributes. If Wj signifies the jth outcome attribute, for example, $\varphi_j$ will be recognized a quality criterion with a quality feature.

$$\varphi_j = Y_{ij}W_1 + Y_{2j}W_2 + \ldots + Y_{jj}W_j \tag{7}$$

where $\varphi_1$denotes the first central component, $\varphi_2$ the second component etc,. Every main component, namely the accountability proportion, specifies several level of explanation of the diversity in performance characteristics. When many major components are layered on top of each other, the accountability steadiness of output attributes progress. It is called total accountability part (CAP).

Step VI: To calculate the combined primary component (CPC) to evaluate multi-composite quality made up of primary components and separate eigen values

$$CPC = \sum_{j=i}^{k} \left( \left| \varphi_j \right|^2 )^1 / 2 \right) \tag{8}$$

The superimposed model is applicable here because all of the major components are independent of one another. A higher CPC number indicates better quality and, as a result, better process performance.

Step VII: To determine the best process parameter settings on output attributes, ANOVA has been performed. Lastly, conduct a confirmation test.

To decrease the idleness and need between the output characteristics, the outputs were normalized by Eqs. (2) and (3). Equations (2) and (3) has been used to normalize MRR and surface roughness (3). The normalized array's variation parameters are then calculated, as illustrated in Table 3. Principle components are concerned for significant output characteristic of the process, which is represented by the proportion of total variance. According to

**Table 4** Analysis of Covariance matrix Eigen values, Eigen vectors, AP, CAP

| | $\varphi_1$ | $\varphi_2$ |
|---|---|---|
| Eigen Vectors | −0.919 | −0.395 |
| | 0.395 | −0.919 |
| Eigen Values | 0.31838 | 0.07987 |
| AP | 0.799 | 0.201 |
| CAP | 0.799 | 1.000 |

Table 4, the primary components for MRR and surface roughness are 79.9% and 20.1 percent, respectively. The individual principal components were calculated by using Eq. (7), as shown in Table 5.The final composite component is consequently found for every experiment by superimposing these individual main components using Eq. (8).

Table 6 shows the computed values of the CPC. As a result, the value provides as an overall quality index of the WEDM process. As a result, the problem is reduced to a single quality optimization problem with maximum CPC, implying higher quality. Finally, an ANOVA was done, as portrayed in Table 7. The corresponding value (P) of each component is shown in the seventh column of Table 7, revealing how it impacted the responses. Based on the ANOVA Ton is the most important measure contributing about 61.38 percent, followed by current (30.35 percent) and Toff (8.26 percent). As a result, Ton is a critical control component to consider when analyzing reactions throughout the WEDM process, followed by current and

**Table 5** Principal components of the performance features

| Experiment number | W1 | W2 |
|---|---|---|
| 1 | 0.226292 | −0.86676 |
| 2 | −0.87785 | −0.37731 |
| 3 | −0.10015 | −0.82561 |
| 4 | −1.95939 | −0.96126 |
| 5 | 0.375112 | −0.91054 |
| 6 | −0.82025 | −0.51133 |
| 7 | −0.28395 | −0.81387 |
| 8 | −0.31411 | −0.32781 |
| 9 | 0.209844 | −0.48822 |
| 10 | −0.393 | −1.12727 |
| 11 | −0.20715 | −1.14379 |
| 12 | −0.524 | −1.314 |
| 13 | −0.18862 | −0.84662 |
| 14 | −0.18862 | −0.84662 |
| 15 | −0.18862 | −0.84662 |

$T_{off}$.

**Table 6** Composite primary components (Overall quality index)

| SL. no | CPC | Rank |
|---|---|---|
| 1 | 0.640 | 13 |
| 2 | 1.255 | 7 |
| 3 | 1.925 | 2 |
| 4 | 1.838 | 3 |
| 5 | 0.535 | 14 |
| 6 | 1.331 | 6 |
| 7 | 1.097 | 8 |
| 8 | 0.641 | 12 |
| 9 | 0.278 | 15 |
| 10 | 1.520 | 4 |
| 11 | 1.350 | 5 |
| 12 | 2.920 | 1 |
| 13 | 1.035 | 9 |
| 14 | 1.035 | 10 |
| 15 | 1.035 | 11 |

## 5 Managerial information, involvement and restrictions

### 5.1 Managerial information

The outcomes are explored in depth in order to provide the following relevant managerial information for effective WEDM:

The established PCA optimization model technique has been tested on novel materials such as Titanium, which is machined using WEDM with cryogenic treated tool. The issue that has been articulated in this research is affected by a combination of variables that have an impact on manufacturing performance, such as RR rises and Ra climbs, which are intrinsically contradictory for industry operators. Researchers are now considering this conflict design and a balance between RR and Ra in order to lower manufacturing costs that are intrinsically linked to profit.

### 5.2 Involvement

The following are among some of the merits of the proposed approach:

- A limit was revealed for how long the solution can be inactive.
- PCA optimum combinations are obtained by minimizing Ra and maximizing RR.

**Table 7** Analysis of variance

| Source | DF | Adj SS | Adj MS | F-Value | *P*-Value | % of contribution |
|---|---|---|---|---|---|---|
| Ip | 2 | 1.09050 | 0.54525 | 2.24 | 0.169 | 30.35 |
| Ton | 2 | 2.20555 | 1.10277 | 4.53 | 0.048 | 61.38 |
| Toff | 2 | 0.29522 | 0.14761 | 0.61 | 0.569 | 8.26 |
| Error | 8 | 1.94835 | 0.24354 | | | |
| Lack-of-Fit | 6 | 1.94835 | 0.32472 | | | |
| Pure Error | 2 | 0.00000 | 0.00000 | | | |
| Total | 14 | 5.57532 | | | | |

### 5.3 Restrictions

Every optimization task, in general, has such restrictions, which are enumerated below:

- The ideal model was only relevant factors and levels, as well as titanium alloy.
- Principal Components attempt to cover as much variance as possible among the features in a dataset; but, if the number of Principal Components is not carefully selected, it may loosing out on some value when opposed to the original list of features.

## 6 Conclusions

The current study proposed an efficient method and framework for optimising WEDM process parameters using titanium alloy zinc coated brass electrode that has been cryogenically treated. On RR and Ra, the proposed approach and framework could provide the optimal process variables. On the output performances, graphs were made for various WEDM settings on the output performances. The following findings were concluded by the study.

On the output performances, graphs for several WEDM parameters were drawn. MRR improves as the pulse time and current grow, as shown in graph. This is described that release large amount of thermal energy is released and maintained for a prolonged period of time, enabling the workpiece surface to melt and vaporise. RR, on the other hand, drops when the pulse is shut off. This is due to fact that when the supply of spark energy is cut off for a prolonged period of time, there is no generation of the conductive route in the IEG, leading to a lower RR.

When the pulse time and applied current rise, Ra grows. Elevated pulse time and current values contribute to increased temperatures and mobility of positive ions in IEG, which strike the electrode surface with high spark energy and generate high temperatures. Enhanced pulse off time, on the other hand, dielectric clears the debris formed during WEDM lowering Ra.

The optimum condition for maximum RR of 0.0602 (mg/min) and minimal Ra of 1.05(μm) in WEDM of Titanium alloy was achieved under the following settings of current 9 amp, On time 120 μs and Off time 200 μs, as determined by PCA. Process variables have a significant impact on outputs, with pulse time having the biggest impact, next by current and pulse off time. Manufacturing engineers can use the optimum condition to calculate an appropriate value for just a few control variables depending on specific procurements, allowing them to considerably enhance production rate by minimizing machining time.

**Acknowledgements** The authors are grateful for the support of the Production Technology Department, MIT,Chennai.

**Author contribution** Dr. C. Senthilkumar, who completed the experiments and wrote the manuscript. Dr. C. Nandakumar, who carried out the analysis.

**Funding** The authors declare that they have no funding of this study.

**Data availability** On request, the dataset used it to facilitate the results of this study can be received from the corresponding author.

**Declarations**

**Conflict of interest** The authors state that there is no conflict of interest.

**Ethical approval** There are no human or animal studies are mentioned in this article.

**Consent to participate** Not applicable.

**Consent to publish** The manuscript does not contain any data from individuals, hence it is not applicable.

## References

Alduroobi AAA, Ubaid AM, Tawfiq MA, Elias RR (2020) Wire EDM process optimization for machining AISI 1045 steel by use of Taguchi method, artificial neural network and analysis of

variances. Int J Syst Assur Eng Manag 11:1314. https://doi.org/10.1007/s13198-020-00990-z
Barenji RV, Pourasl HH, Khojastehnezhad VM (2016) Electrical discharge machining of the AISI D6 tool steel: prediction and modeling of the material removal rate and tool wear ratio. Precis Eng 45:435–444
Bharat C, Khatria Pravin P, Rathod J, Valaki B, Sankhavara CD (2017) Insights into process innovation through ultrasonically agitated concentric flow dielectric streams for dry wire electric discharge machining. Mater Manuf Process 33:1438–1444
Chalisgaonkar R, Kumar J (2014) Parametric optimization and modeling of rough cut WEDM operation of pure titanium using grey-fuzzy logic and dimensional analysis. Cogen Eng 1(1):1–28
Datta RS, Biswal BB (2019) Experimental studies on electro- discharge machining of Inconel 825 super alloy using cryogenically treated tool/workpiece. Measurement 145:611–630
Goswami A, Kumar J (2014) Investigation of surface integrity, material removal rate and wire wear ratio for WEDM of Nimonic 80A alloy using GRA and Taguchi method. Eng Sci Technol Int J 17(4):173–184
Goyal A (2017) Investigation of material removal rate and surface roughness during wire electrical discharge machining (WEDM) of Inconel 625 super alloy by cryogenic treated tool electrode. J King Saud Univ Sci 29:528–535
Hasani A, Mokhtari H, Fattahi M (2021) A multi-objective optimization approach for green and resilient supply chain network design: a real-life case study. J Clean Prod 278:123199
Hotelling H (1933) Analysis of a complex of statistical variables into principal components. J Educ Psychol 24(6):417–441
Jabbaripour B, Sadeghi MH, Faridv S, Shabgard MR (2012) Investigating the effects of EDM parameters on surface integrity MRR TWR Machining Ti–6Al–4V. Mach Sci Technol 16:419–444
Kapoor J, Singh S, Khamba JS (2015) Effect of cryogenic treated brass wire electrode on material removal rate in wire electrical discharge machining. J Mech Eng Sci 226(11):2750–2758
Kumar S, Batish A, RupinderSingh., AnirbanBhattacharya., (2017) Effect of cryogenically treated copper-tungsten electrode on tool wear rate during electro-discharge machining of Ti-5Al-2.5Sn alloy. Wear 386–387:223–229
Nayak BB, Mahapatra SS (2016) Optimization of WEDM process parameters using deep cryo-treated Inconel 718 as work material. Eng Sci Technol Int J 19:161–170
Oliver-Nesa-Raj S, Prabhu S (2017) Modeling and analysis of titanium alloy in wire-cut EDM using grey relation coupled with principle component analysis. Aust J Mech Eng 15(3):198–209
Pearson K (1901) On lines and planes of closest fit to systems of points in spaces. Philos Mag Ser 2:559–572
Rajesh S, Sharma AK, Kumar P (2012) On electro discharge machining of Inconel 718with hollow tool. J Mater Eng Perform 21(6):882–891
Senthilkumar C, Ganesan G (2015) Electrical discharge surface coating of EN38 steel with WC/Ni composite electrode. J Adv Microsc Res 10:202–207
Tahir W, Jahanzaib M (2019) Multi-objective optimization of WEDM using cold treated brass wire for HSLA hardened stee. J Braz Soc Mech Sci Eng 41:525–539
Torres A, Luis CJ, Puertas I (2017) EDM machinability and surface roughness analysisof $TiB_2$ using copper electrodes. J Alloys Compd 690:337–347
Vázquez-Méndez ME, Casal G, Castro A (2020) Optimization of an urban railway bypass. A case study in a Coruña-Lugo line Northwest of Spain. Compd Ind Eng 151:106935
Walia RS, Shan HS, Kumar P (2006) Multi-response optimization of CFAAFM process through Taguchi method and utility concept. Mater Manuf Process 21:907–914